Interdiscip Sci Comput Life Sci (2018) 10:93–104
https://doi.org/10.1007/s12539-016-0170-y

ORIGINAL RESEARCH ARTICLE

Binding Patterns Associated Aß-HSP60 p458 Conjugate to HLA-DR-DRB Allele of Human in Alzheimer's Disease: An In Silico Approach

Naveen Padmadas[1,2] · Pritam Kumar Panda[1] · Sudarsanam Durairaj[3]

Received: 9 October 2015 / Revised: 5 April 2016 / Accepted: 7 April 2016 / Published online: 23 April 2016

Abstract Alzheimer's disease (AD) is a complex, irreversible, progressive brain disorder, which diminishes memory in a slow pace and thinking skills; ranked third by experts. It is a complex disorder that involves numerous cellular and subcellular alterations. The pathogenesis of AD is still unknown, but for better understanding, we proposed an in silico analysis to find out the binding patterns associated with HSP60. Several experimental conclusions have been drawn to understand the actual mechanism behind the forming of aggregation due to misfolding. Protein misfolding disorder is experimentally identified by the accumulation of protein aggregates at the intracellular or extracellular region of brain that adversely affects the cell functioning by disrupting the connection between the cells and ultimately leading to cell death. To unravel the mystery behind the mechanism of AD through computational approach, the current proposal shows the designing of Aß-HSP60 p458 conjugate followed by secondary structure analysis, which is further targeted to HLA-DR-DRB allele of human. The antigenicity of Aß (1–42) peptide is the major concern in our study predicted through PVS server, which provides an insight into the immunogenic behavior of Aß peptide. The mechanism involved in the interaction of HSP60-Aß conjugate with HLA-DR-DRB allele considering the fact that Aß (1–42) is highly immunogenic in human and interactions evoked highly robust *T*-cell response through MHC class II binding predictions. It was assisted by molecular dynamics simulation of predicted HSP60 structure followed by validation through Ramachandran plot analysis and protein–protein interaction of Aß (1–42) with HSP60.

Keywords Heat shock protein 60 (HSP60) · Amyloid beta · Alzheimer's disease · HLA-DRB1 · Aß-HSP60 peptide · Gromacs · Cluspro · UCSF chimera

Abbreviations

AD	Alzheimer's disease
HSP60	Heat shock protein
Aß	Amyloid Beta
Aß-HSP60	Amyloid Beta (1–15)-heat shock protein (p458–474)
HLA-DRB1	HLA class II histocompatibility antigen, DRB1-1
MHC class II	Major histocompatibility complex class II
H-Bond	Hydrogen bond
A	Acceptor
D	Donor
Å	Angstrom

1 Introduction

Alzheimer's disease (AD) is a neurodegenerative disorder in which your brain undergoes an irreversible deterioration causing disruption in memory and other functions and

Electronic supplementary material The online version of this article (doi:10.1007/s12539-016-0170-y) contains supplementary material, which is available to authorized users.

✉ Naveen Padmadas
naveenpadmadas@gmail.com

[1] School of Biotechnology and Bioinformatics, D. Y. Patil University, CBD Belapur, Navi Mumbai, Maharashtra 400614, India

[2] Research and Development Centre, Bharathiar University, Coimbatore 641 046, India

[3] Department of Advanced Zoology and Biotechnology, Loyola College, Chennai 600 034, India

finally resulting in death from complete brain failure. The 2015 AD facts and figures suggest this as the only cause of death in the top ten in America that can neither be prevented, cured or slowed down. An alarming figure of one in every three senior citizens in America dies of AD or dementia and two in every three individual diagnosed with AD are females. An estimate of 700,000 people in the United States of age 65 and older will die in the year 2015 with AD (http://www.alz.org/). Although we do not know when the process of AD begins in an individual, it is understood that the problem begins a decade or more before the first evidence. New brain imaging techniques have given information about abundance of two abnormal structures: amyloid plaques and neurofibrillary tangles which are made of misfolded proteins in AD patients. (Alzheimer's Disease—Unraveling the Mystery—www.nia.nih.gov/alzheimers). Another aspect of AD is the disruption in the connection between cells, which adversely affects the cell function leading to cell death. This disorder, otherwise known as "*protein misfolding disorder*", is identified by the accumulation of protein aggregates at the intracellular or extracellular region [1]. Some of these protein aggregates, which contain large number of intermolecular hydrogen bond, sometimes get converted to a fibrillar structure commonly called as amyloid or beta amyloid—a misfolded structure and their accumulation makes it a plaque like structure [2]. This is observed in regions of the brain that are important in memory.

Beta amyloid (Aβ) is the peptide with 39–42 amino acids and is the major component of the amyloid plaques found in the brains of Alzheimer's patients. This peptide is an outcome from the amyloid precursor protein (APP) by the proteolytic activities of β- and γ-secretase to produce Aβ [3, 4]. Review of literature suggests that in AD patients Aβ (1–42), fragment is the dominant one in Aβ species when compared to Aβ (1–40) in the formation of amyloid plaques. The in vitro *studies* displayed a dramatically increased inclination to form amyloid fibrils [5–7]. Numerous significant structural features of Aβ (1–42) fibrils have been dogged founding that Aβ (1–42) fibrils form a cross-β structure that contains parallel, in-register β-sheets [8–10]. Molecules of Aβ aggregate to form flexible soluble oligomers and may exist in several forms. We have enough reasons to believe that certain misfolded oligomers act as seeds and induce other Aβ molecules to take the misfolded oligomer form. This leads to a chain-like reaction similar to a prion infection. These seeds or the consequential amyloid plaques are lethal to the nerve cells. Tau protein, the other protein associated in AD, also forms such prion-like misfolded oligomers, and there are some evidences that the misfolding in tau is induced by Aβ [11, 12]. The plaques are a collection of a mass of regularly ordered fibrillar aggregates called amyloid fibers [13]. Latest research recommends that soluble oligomeric forms of the peptide may be instrumental in the development of AD [14, 15]. Recent studies suggest that this kind of protein aggregation in AD can be mainly caused by two factors: The misfolded proteins get accumulated between the neurons and cause disease. Secondly, this can happen because of aging resulting in decrease in proteasomal activity and alteration in the functional capacity of molecular chaperones [1]. Molecular chaperones are a class of cellular protein that plays an integral role on other proteins assisting them in their interaction, stabilization and acquiring functional conformations and leave the protein [16]. One of the major classes of molecular chaperones is heat shock proteins (HSP). Although the name says heat shock, HSPs are induced by cells in response to bacterial and viral infection, chemical exposure, deficiency of nutrition, necrosis in mammalian hosts, UV irradiation and oxidative stress [17]. HSPs are phylogenetically conserved proteins and are named according to their approximate molecular weight: HSP10, HSP40, HSP60, HSP70, HSP80 HSP90 etc. One of the most important functions of HSP is to bind with non-native proteins and assist them in acquiring their native structure and restrict them from misfolding and aggregation process. Investigation on the role of these proteins in neurodegenerative diseases revealed that they provide a basic level of defense against misfolding and are among the most potential suppressors of neurodegeneration in animal and cellular models [18, 19]. Several investigational findings have thrown light on the fact that overproduction of some HSPs can lead to the defense of numerous disease conditions including neurodegeneration progression and disease-related toxicity [20]. Latest studies have revealed that HSPs were found to be localized in protein aggregates along with cellular molecules, diseased proteins and ubiquitin. Conclusions were drawn that the HSPs probably attempted to revert the refolding of misfolded proteins or it attempted to revert the mutational effects of the gene, thus trying to suppress the disease condition; however, the mechanism is poorly understood [1]. Lately, several HSP modulators have testified to activate the solubilization of unhealthy protein aggregates. Therefore, HSPs are an excellent choice for therapeutic targeting and very likely to have strong prospective as therapeutic agents in suppressing or curing neurodegenerative disease like AD [1].

Among the various classes of HSPs, HSP60 under normal physiological conditions is an oligomer consisting of monomers arranged as two stacked complex heptameric ring [21]. This is localized to cytoplasm and mitochondrial region, and its major function is to prevent protein aggregation and to help proper folding of proteins [1]. The unfolded protein binds through hydrophobic interactions in the large cavity of the double-ring structure of HSP60 [22].

The HSP60 structure comprises of an apical domain, intermediate domain and equatorial domain. The ATP binds to the equatorial domain. The binder for equatorial and apical domains is the intermediate domain. The protein is in a hydrophobic state when inactive and the intermediate domain undergoes a conformational change when activated by ATP, which results in exposing the hydrophilic region. This assures reliability in protein binding. HSP10 supports HSP60 in folding by acting as a dome-like cover on the ATP active form of HSP60 resulting the central cavity to enlarge and help in protein folding [23].

Recently, Aβ-HSP60 conjugate vaccine was found to be effective in treating a mouse model of AD [24] Immunization with the conjugate resulted in the initiation of Aβ-specific antibodies resulting in a significant reduction in the amount of amyloid in animal model brain. This positive result encouraged testing in humans. Approximately 6 % of the vaccinated AD patients showed development of meningoencephalitis, and the human clinical trial of the active Aβ was stopped. Investigations to find out the reason for the development of pathogenic *T* cells attributed to the use of QS21, a very strong adjuvant and the full length of the Aβ. But, the positive results have encouraged putting in further efforts to refine the Aβ immunotherapy to produce safer vaccines for AD [24, 25].

In this current study, we have intensely studied the molecular dynamics of the Aβ-HSP60 conjugate up to 20 ns at variant time intervals, respectively. This can give us further insight into the sequential shifts if any and changes in the structural conformation of the conjugate. This study enlightens the Aβ-HSP60 conjugate as a potential therapeutic target.

2 Methods

2.1 Sequence and Structure Retrieval, Homology Modeling

The HSP60 sequence of *Homo sapiens* with UniprotKB [26] Accession number P10809 containing 573 amino acids was retrieved. More information about the protein was taken from Structural Classification of Protein database [27] and Superfamily 1.75. As there was no human HSP60 structure reported in Protein Data bank [28], homology modeling was carried out to model the structure. Keeping human HSP60 as the query sequence, BLAST [29] with Blosum62 substitution matrix against PDB database and default parameter was carried out to find the homologous template. After investigating the missing residues and resolution, a potential template with PDB id 1IOK was selected. Further, homology modeling using SWISS-MODEL server was carried out in automatic mode [30, 31]. The NMR solution structure of the Alzheimer's disease Aß-peptide (1–42) was retrieved from RCSB PDB and used as the potential target in our study.

2.2 Structure Validation

Validation of the generated model was carried out using protein structure analysis (ProSA-web) tool [32, 33] and Structural Analysis and Verification Server (SAVES-Ramachandran Plot). The tools gave an understanding of the residual clashes [34]. Molecular graphics and analyses were performed with the UCSF Chimera package [35].

2.3 Molecular Dynamics

Molecular Dynamics simulation is a vital aspect to interpret the intrinsic molecular levels of several proteins. The approaches involved in understanding the atomistic level of the protein have been simplified by molecular dynamics. In our current study, the molecular dynamics simulation is used to study the functional and stability aspect of the modeled HSP60 protein. The modeled protein was exposed to dynamics study under solvent (water) environment using Gromacs 4.5.5 version [36–41].

The energy minimization of the protein was done using OPLS-AA/L (optimized potentials for liquid simulations—all-atom force field) (2001 amino acid dihedrals). The topology file thus created defines other molecules and provides system-level descriptions. The default force constant is used to keep atoms in place during equilibration, which is further illustrated during equilibration phase.

The grid preparation was done using SPC/E (extended simple point charge model) solvent model. The protein with added ions was centered in a cubic box of dimension specifying a solute-box distance of 1.0 nm with SPC/E water molecules. Four cl- ions were added as counter ions to neutralize the charges in the system using steepest descent minimization with 50,000 steps. The solvated, electroneutral system generated is then confined to a periodic box. This was subjected to energy minimization for 5000 steps (10 ps) with steep integrator using steepest descent algorithm and continued till the potential energy was converged and stabilized. The equilibrium state of the system was achieved by keeping temperature and pressure constant for 100 ps (50,000 steps) using modified Berendsen Thermostat t-coupling algorithm and Parrinello-Rahman pressure coupling parameter. The system components were separately coupled to a temperature bath at 300 K with a coupling time constant of 0.5 ps. The short-range van der Waals and electrostatic cutoff was set to 1.2 nm. Long-range electrostatic interactions were calculated using the particle mesh Ewald (PME) method. Semi-isotropic pressure coupling was carried out using a Berendsen barostat,

and the volume compressibility was chosen to be 4.5610 bar.

Comparative simulation study has been carried out with 20 ns to comprehend the structural orientation of the binding site as well as to reinstate the current finding in our research. The leapfrog integrator was used for integrating Newton's equation in MD simulation. Linear constraint solver algorithm was used on protein covalent bonds to maintain constant bond lengths. The constraint algorithm LINCS (linear constraint solver): holonomic constraints were applied to the equilibrated protein to release the atomic constraints previously defined. Grid-type neighbor searching was applied, and long-range electrostatics was handled using PME (particle mesh Ewald). Finally, the equilibrated system was subjected to MD simulations at 300 K and all atoms were permitted to move freely for the purpose of studying the stability and its conformations.

2.4 MatchMaker

MatchMaker from the tool chimera was used for superimposing protein structures by first creating pairwise sequence alignments, then fitting the aligned residue pairs using one point per residue. A structure-based multiple sequence alignment was also computed after the structures have been superimposed. In our present study, the HSP60 protein, which was subjected to MD simulation at different time intervals, was compared in a sequential perspective using residue pair shifting with default parameters. The iteration by pruning long atom pairs until no pair exceeds $x = 2.0$ Armstrong was used to superimpose the structures. This tends to exclude sequence-aligned but conformational dissimilar regions such as flexible loops, allowing a tighter fit of the best-matching "core" regions [42].

2.5 Protein–Protein Interaction

Protein–protein interaction of HSP60- Aβ conjugate was carried out using Cluspro 2.0 server. [43–46]. Cluspro is a fully automated web-based program used for rigid protein–protein docking. Users have the choice of uploading the PDB files from local machine or directly from PDB server (http://www.rcsb.org/pdb/) database. The algorithm used in Cluspro 2.0 is based on fast Fourier transform using continuum electrostatics and geometric fit (DOT) [47] or a novel shape complementarity scoring function for protein–protein docking (Z-DOCK) [48] to perform rigid body docking. After processing the files, the docking algorithm evaluates multiple number of conformations retaining the most favorable interactions provides a choice to choose from balanced, electrostatic-favoured, hydrophobic-favoured and VdW + electrostaic-favoured interactions. The working of the Cluspro server is based on rotation of the ligand (protein) with 70,000 rotations relative to the receptor grid, and greedy clustering of the filtered 1000 interacted structures out of 70,000 rotations is based on positioning of ligand (protein) with 9 Å C-alpha RMSD radius until final 30 models were generated. The simulated HSP60 protein as receptor and amyloid beta (Aβ) (1–42) as a ligand were subjected to Cluspro 2.0 server with default docking parameters. The prediction used in this study was based on balanced interactions, which gave 30 interactions, out of which the most favorable interaction was the 0th model with lowest energy of −790.0 and 71 cluster sizes.

2.6 Peptide Designing and Validation

Literature review suggested the peptide amyloid beta (Aβ) (1–42) is highly immunogenic in humans. This was experimentally validated using mouse models carrying DRB1*1501 allele, which evoke *T*-cell response [24]. Protein Variability Server (PVS) was used to predict the antigenicity of the peptide amyloid beta (Aβ) (1–42). This method uses Kolaskar and Tongaonkar algorithm [49] based on occurrence of amino acid residues in experimentally determined epitopes. This generates an antigenic plot based on average antigenic propensity.

2.7 MHC Class II Binding Prediction

MHC class II proteins are expressed only on APCs (antigen presenting cells) that form epitopes recognized by *T*-helper cells ($CD4^+$) and are involved in response to all antigens. Several conformations of peptides bound to MHC class II molecules that are having variable lengths bind to both N- and C-terminal ends. The study has been conducted in our research on the basis of the involvement of MHC class II molecules in binding to variable lengths of peptides in response to small fragments of antigen, which evoke a *T*-cell response. The MHC binding peptide prediction helps in finding a range of peptides defined by the property named MHC allelic polymorphism. The method used in our predictions was based on mathematical expression-based neural network approach in which the predictive accuracies are higher in comparison with other motif-based analysis and structure-based methods [50]. In this study, peptide designing of Aβ (1–15)—HSP60 (p458–474) was carried out using UCSF Chimera. Computational approaches were further used to study the effect of the constructed peptide and their interactions in human HLA. MHC class II Binding Peptide Prediction Server was used to check the residue binding positions [51]. This server helps in predicting the MHC class II binding regions in antigenic sequences.

3 Results and Discussion

3.1 Structure Validation

The assessment by Procheck server for the predicted structure gave 90.3 % residues in favorable region, 7.6 % in additional allowed region, 1.1 % in allowed and 1.1 % in disallowed region, which thus inveterate to be a good structure for further analysis. The native conformation was validated by PROSA, showing an overall model quality with a Z score of −11.27 (Figs. 1, 2, 3).

3.2 Structure and Dynamics

An MD simulation of the modeled HSP60 protein was performed for 20 ns in solvent environment to ensure adequate testing. The structural variation during the course of the simulation was observed to be 0.4–0.5 nm and is shown in the RMSD plot (Fig. 4). The structure is considered stable.

3.3 MatchMaker

A search in BlastP for finding out conserved domains in HSP60 resulted in residues numbering 28–548 as conserved and showed GroEL like Type 1 chaperonin activity. This was further aided by MatchMaker tool using the residual-based comparison as shown in the supplementary files (S1: Fig. 1). The domain corresponding to the interaction with the beta amyloid, which was further implicated in our study, plays a significant role for the binding efficacy of the conjugate. The residues in comparison with wild type vary much significantly in 20 ns at C-terminal positions, but the functional binding domain region of our interest remains the same and conserved.

Fig. 1 Representation of HSP60 structure using UCSF Chimera showing N- and C-terminal region

3.4 Protein–Protein Interaction Analysis: HSP60-Aß Conjugate

Hydrogen bonds play a vital role in predicting the interactions, shapes and properties of biomolecules [14, 15]. These are the non-covalent interactions between the

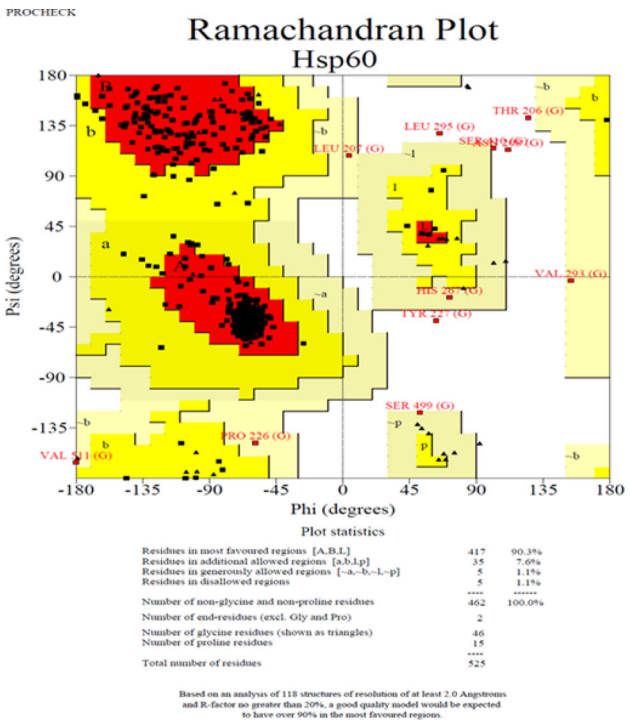

Fig. 2 Structural validation using procheck (Ramachandran plot analysis)

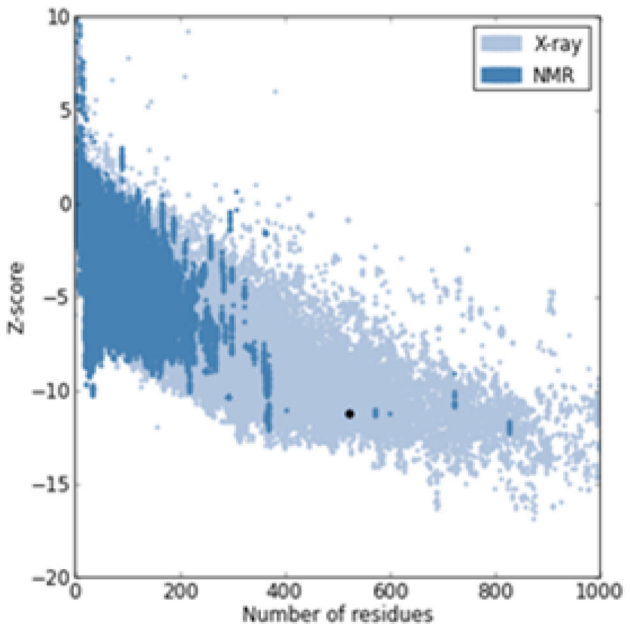

Fig. 3 Validation of HSP60 predicted structure using PROSA

hydrogen bond acceptors and donors, which determine the strength. The formation of intermolecular hydrogen bonds is observed between D…A and D–H…A. The mean hydrogen bonds distances in protein secondary structures are close to 3.0 Å according to Watson and Crick pairing model. According to Jeffrey [52], the strong hydrogen bonds with D…A distance are 2.2–2.5 Å, mostly covalent, 2.5–3.2 Å as moderate, mostly electrostatic and 3.2–4.0 Å as weak, electrostatic. The hydrogen bonding pattern of the conjugate (Fig. 5) shows a strong interaction of salt bridges formed between Arginine 141 and lysine 352 with glutamic acid 11 and aspartic acid 23, respectively, as shown in (Figs. 6, 7; Table 1). The resulted hydrogen bonding interaction pattern was generated using LigPlot^{+} [53] version 1.4.5 using DIMPLOT for protein–protein interaction.

3.5 Peptide Designing

Generally, the N- and C- terminal regions of proteins are usually solvent accessible and unstructured, Abs against those regions are also likely to recognize the native protein and are antigenic in nature. So, through computational approaches, the Aß-HSP60 conjugate was designed and visualized using UCSF Chimera as shown in (Fig. 8). N-terminal region of Aß peptide (1–15) and C-terminal region of HSP60 (p458–474) were conjugated using structure-editing tool in chimera where the designing of peptide with default φ (phi) and ψ (psi) angles i.e., φ (°) −57 and ψ (°) −47 of alpha helix conformation and Dunbrack [54] rotamer library were chosen (default parameters). The rotamer at each position will be evaluated as by the fewest number of clashes. The residues are added in N → C order and assigned a specified chain ID. The constructed peptide Aß-HSP60 conjugate was subjected to minimization using minimize tool in chimera. The default algorithm, i.e., steepest descent (10,000 steps) with a step size of 0.02 Å and conjugate gradient (100 steps) with step size of 0.02 Å, was applied for minimization. Further analyses were done using the minimized peptide Aß-HSP60 conjugate.

The secondary structure conformation of the peptide was depicted in (Table 2) which was done using SOPMA [55] secondary structure prediction server.

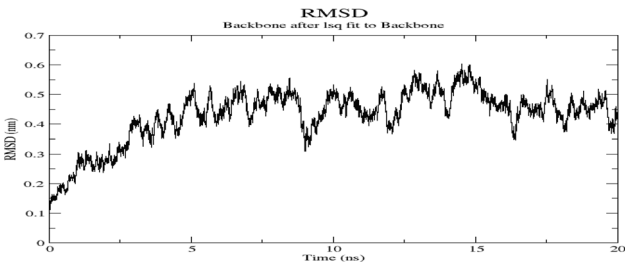

Fig. 4 RMSD plot of HSP60 after 20 ns simulation using Gromacs 4.5

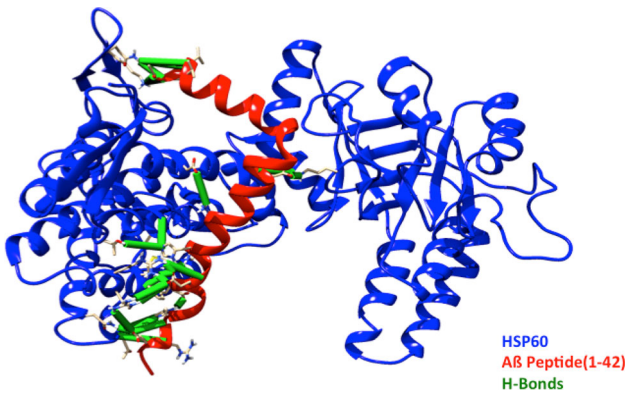

Fig. 5 Protein–protein interaction between HSP60 and Aß (1–42) peptide

3.6 Antigenic Site Prediction

The antigenic sites prediction of Aβ-HSP60 conjugate was done using Protein Variability Server. The average antigenic propensity was 0.9963, and it returned two antigenic peptides as shown in (Fig. 9). The graph plotted clearly indicates that the peptide sequence SGYEVHH (8–14) of Aβ was more antigenic than that of HSP60 (21–27) region.

3.7 MHC Class II Binding Prediction

The constructed Aß-HSP60 peptide was subjected to MHC class II binding prediction and Rankpep [56] to analyze the MHC binding affinity of the peptide. On the basis of these results, the peptide of interest that is antigenic in nature can be proposed as a vaccine candidate. Table 3 shows the predicted peptides of Aß-HSP60 conjugates, which are having binding efficacy to MHC class II in which the third peptide IGIEIIKRT (20–28) shows highest binding affinity with a score of 9.69. The allele used was HLA-DRB1*1501 which was also used in experimental methods in mice models. The Rankpep server predicts the binding peptides based on position-specific scoring matrices (PSSMs). In addition, it predicts those MHC ligands whose C-terminal end is likely to be the result of proteasomal cleavage. On the basis of the function of MHC class II molecule, the Rankpep server returns a peptide VHHQNEDQK (12–20) that is most likely present in C-terminal region of Aß-HSP60 peptide.

Each peak in the graphical view plot (Fig. 10) depicts the binding affinity of peptide in each peptide frame comes

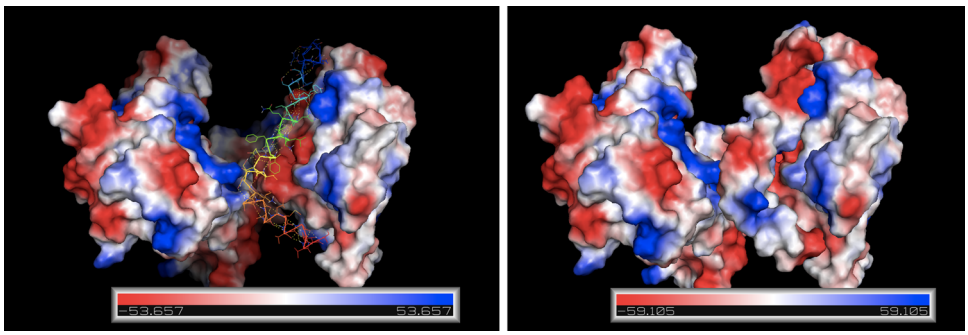

Fig. 6 Electrostatic potential computed by Pymol showing hydrophobicity scale of the conjugate HLA-HSP60-Aß Complex. *Red* represents negative charged residues, and *Blue* represents positively charged residues

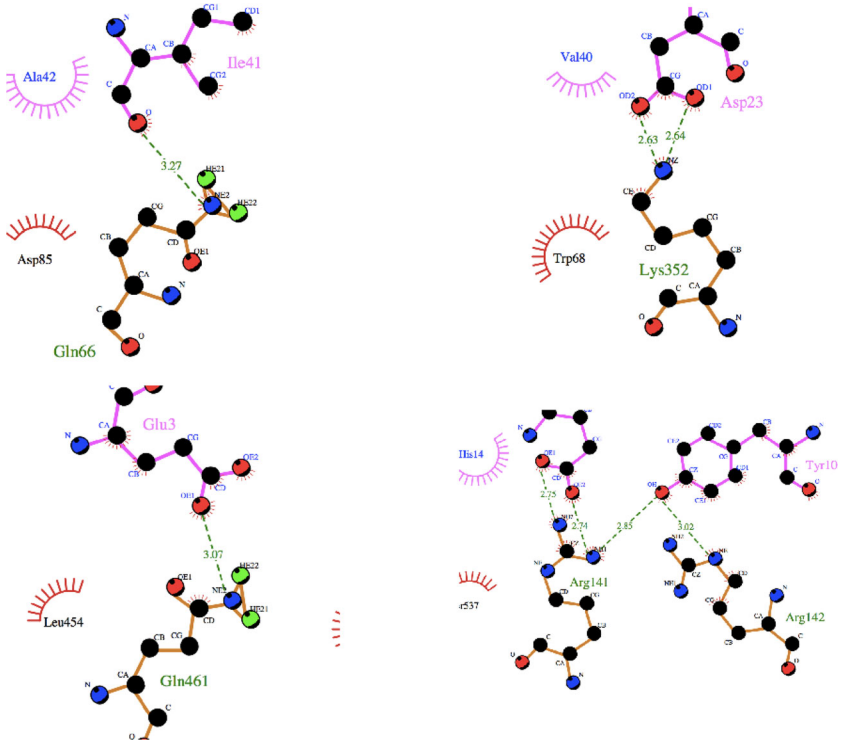

Fig. 7 Residue interaction plot of Aß (1–42) involved in hydrogen bonding with HSP60 using LigPlot^{+} (v1.4.5)

Table 1 Hydrogen bonding interaction between amyloid beta (1–42) and HSP60

HSP60	Atom involved (Donor)	H-Bond distance D…A	Amyloid beta (1–42)	Atom involved (Acceptor)	H-Bond distance D–A…H	Bond angle D–A…H
GLN 66	NE2	3.27	ILE 41	O	2.304	12.98°
ARG 141	NH1	2.74	GLU 11	OE2	2.085	30.06°
ARG 141	NH2	2.75	GLU 11	OE1	1.773	31.14°
ARG 141	NH1	2.85	GLU 11	OH	1.866	45.11°
ARG 142	NE	3.02	TYR 10	OH	2.114	21.01°
LYS 352	NZ	2.63	ASP 23	OD2	1.781	29.04°
LYS 352	NZ	2.64	ASP 23	OD1	1.793	27.36°
GLN 461	NE2	3.07	GLU 3	OE1	2.093	12.43°

under the score distribution profile. This profile provides the magnitude of the binding affinity of each peptide that is helpful in finding the promiscuous binders which correlates to the immunogenicity of each peptide. The peaks under the dashed lines (blue color) are predicted as the promiscuous binders. The threshold profile is plotted on a scale of

threshold vs. number of peptide frames that are helpful in selecting peptide binders. A peak crossing dashed line (red color) in threshold profile depicts the predicted binders plotted on *Y*-axis (peptide frame score), which can be reflected in antigenic sequences [50].

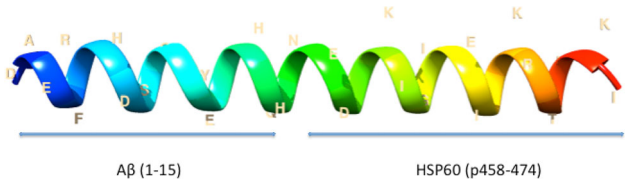

Fig. 8 Aβ (1–15)–HSP60 (p458–474) conjugate peptide

3.8 Protein–Protein Interaction of Aß-HSP60 Peptide with HLA-DRB-1 Allele of Human

HLA-DRB1 (HLA class II histocompatibility antigen, DRB1-1) is a human allele of MHC class II that binds to peptides, which are antigenic in nature for recognition of CD4 *T* cells through endocytic pathway. The binding site of HLA can accommodate 10–30 residues. Aß-HSP60, thus immunogenic to human acts as an antigen, which further can be degraded through several degrading enzymes. Thus, the antigens that are presented to MHC class II molecules undergo proteolysis due to high lysosomal environment. In our current research, protein encoding the HLA-DRB1 gene has been retrieved from

Table 2 Secondary structure analysis of the peptides

Structures	Alpha helix (%)	Beta turn (%)	Extended strand (%)	Coils (%)
Amyloid beta peptide (1–42)	4.76	19.05	52.38	23.81
Amyloid beta (1–15)	0	0	0	100
HSP60 (p458–474)	70.59	0	5.88	23.53
Aß-HSP60 conjugate	34.38	9.38	21.88	34.38

Fig. 9 Antigenic site prediction

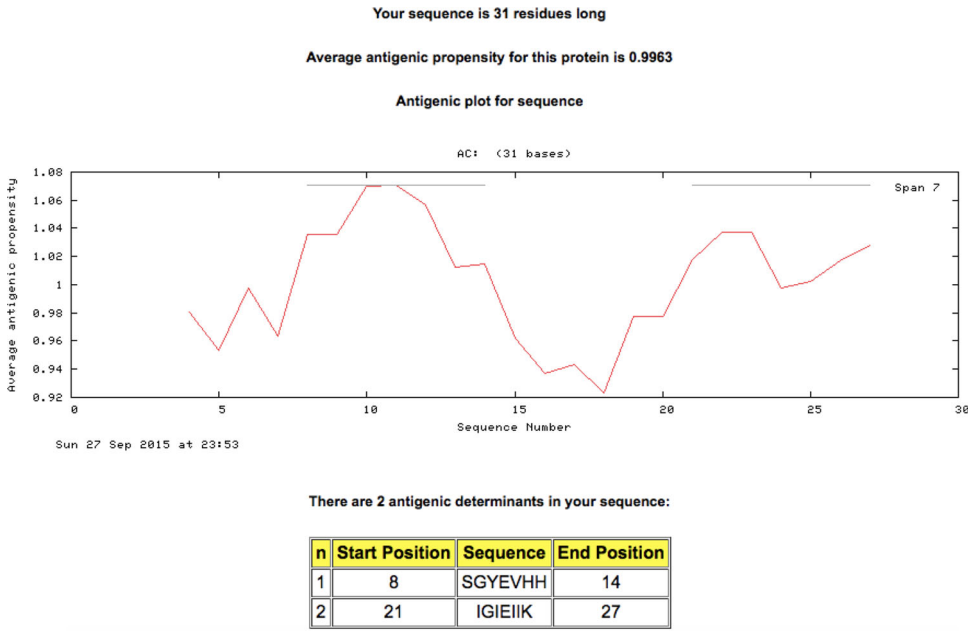

Table 3 Ranking of peptides based on binding efficacy to MHC class II

Rank	Sequence	At position	Score	% of highest score
MHC class II binding prediction server				
1	FRHDSGYEV	3	2.5000	25.51
2	IEIIKRTLK	22	1.7000	17.35
3	IGIEIIKRT	20	0.9500	9.69
Rankpep Server				
4	VHHQNEDQK	12	10.505	25.11

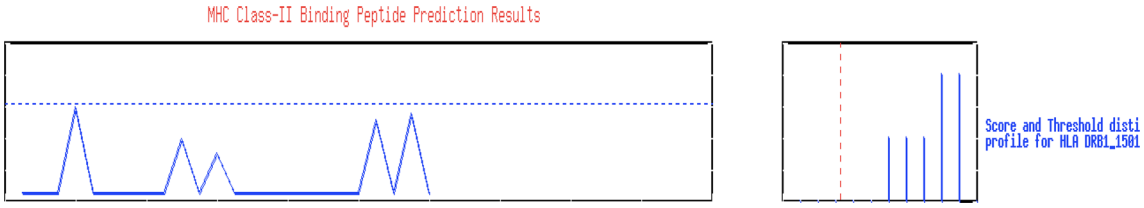

Fig. 10 Aß-HSP60 conjugate binding to MHC class II. The *rectangular box* represents score distribution profile, and the *square box* represents the threshold profile

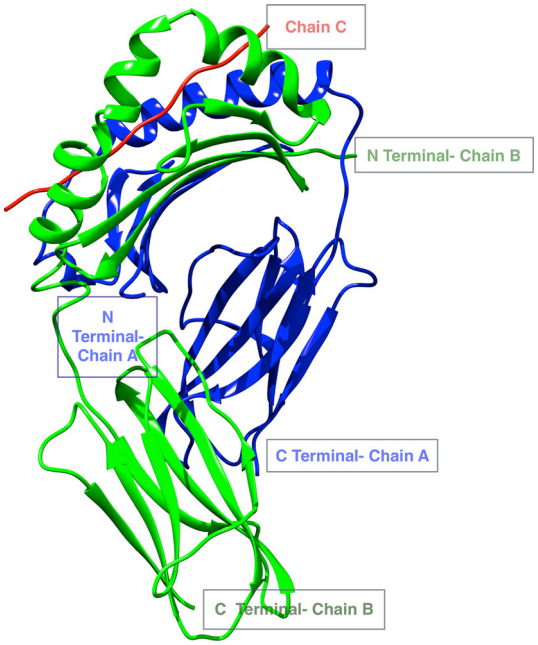

Fig. 11 Structure of HLA-DRB1 showing N- and C-terminal regions. (*Blue* represents Chain A, *Green* represents Chain B, *Red* represents Chain C)

Protein Data Bank [PDB ID-1AQD (2.45Å)] as shown in (Fig. 11) that is having function of antigen processing and presenting [57]. Computationally constructed peptide Aß-HSP60 was subjected for protein–protein interaction with HLA-DRB1 allele of human using Cluspro 2.0 server. The default parameters were used as discussed earlier in Materials and Method section. The interaction resulted in 30 binding interactions out of which the lowest energy interaction with 794.9 and cluster member of 242 was selected. The interaction stemmed in binding of peptides predicted from MHC class II binding server and Rankpep. The residues LYS27, LYS31, GLN19, ASN16 and LEU30 interacted with HLA-DRB1 allele implicates that most of the residues are from C-terminal region of the antigenic peptide (Fig. 12), and the hydrogen bonding analysis was depicted in (Table 4) with H-bond distance and atoms involved in the interaction using Chimera H-bond analysis tool and Ligplot^{+}.

4 Conclusion

This study focuses on the structural perspective of Aß (1–42) peptide, which is considered as an antigenic to human cells. The utilization of Aß (1–42) peptide has several immunodominant epitopes that were experimentally validated using mice models with different genetic backgrounds. The HSP60 model was predicted using Swiss-Model server and was validated using Ramachandran plot in which most of the residues were in mostly favorable regions. In the line of study, Aß interaction with HSP60 concentrates on post-translational modifications and folding process, which necessarily do not occur in case of Alzheimer's disease. Since the formation of electrostatic bonds with hydrogen bonds depicted the strong interaction of the Aß with HSP60, the mechanism underlying the concept is still a mystery. As per experimental data provided by Nemirovsky et al. tested in mice models, the concept of vaccine development against the aggregation of the peptide Aß was proposed and tested. The employment of Aß (1–42) for vaccine development computationally was implemented in our work. In structural perspective, the AD vaccine was modeled using N-terminal region of Aß (1–15) peptide conjugated with HSP60 (p458–474). To check the antigenicity of the modeled Aß-HSP60 peptide, server-based predictions were applied to identify the most antigenic sites based on average propensity. Several peptide regions were predicted as antigenic based on different algorithms. According to the literature review, several epitopes in humans were mostly in C-terminal regions and were HLA-DR dependent of MHC class II cells. HLA-DRB1 (HLA class II histocompatibility antigen, DRB-1) is a human allele of MHC class II that binds to peptides, which are antigenic in nature for recognition of CD4 *T* cells through endocytic pathway. To justify the concept of antigenicity and dependency on HLA-DB in human cells, protein–protein interactions was carried out between HLA-DRB1 and Aß-HSP60 peptide which is responsible for evoking *T*-cell responses in human cells through endocytic pathway. The human allele HLA-DRB1-1501 was used in MHC binding peptide server, which resulted in prediction of C-terminal regions of the Aß-HSP60 peptide. This was achieved by protein–protein interaction of HLA-DRB1

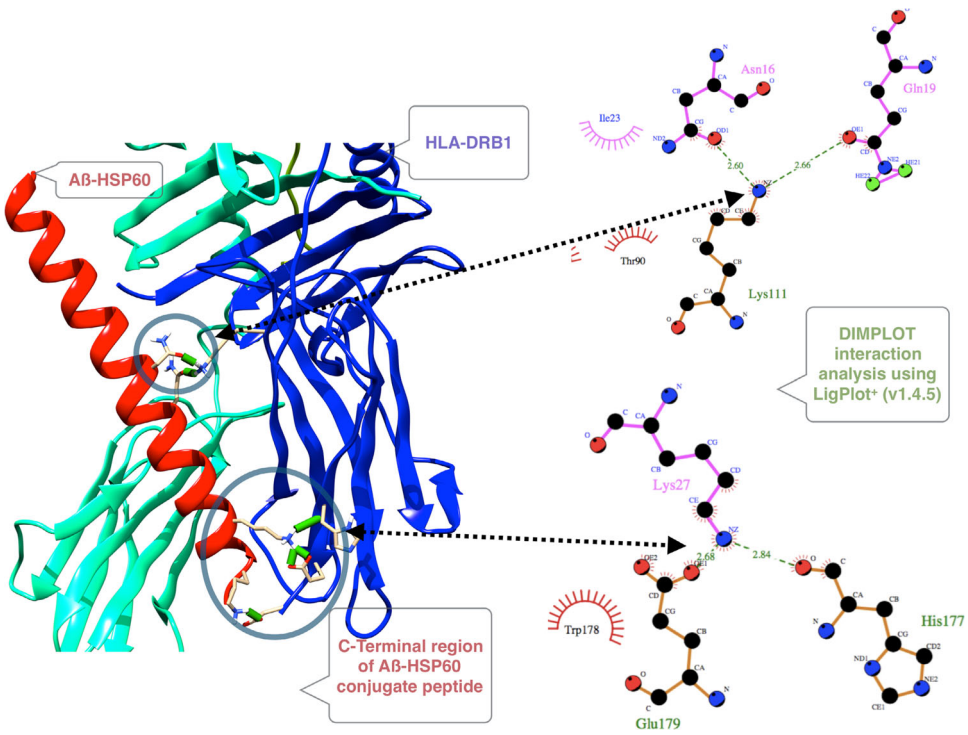

Fig. 12 Interaction of Aß-HSP60 conjugate with HLA-DRB1

Table 4 H-bond interactions between Aß-HSP60 with HLA-DRB1

Aß-HSP60 conjugate peptide	Atoms involved	H-bond distance D….A	H-bond distance D–H…A	HLA-DRB1	Atoms involved
LYS 27	NZ (Donor)	2.839	1.845	HIS 177 (Acceptor)	O
LYS 27	NZ (Donor)	2.683	1.748	GLU 179 (Acceptor)	OE1
LYS 27	NZ (Donor)	2.619	1.858	GLU 179(Acceptor)	OE2
ASN 16	OD1 (Acceptor)	2.604	1.704	LYS 111 (Donor)	NZ
GLN 19	OE1 (Acceptor)	2.660	1.733	LYS 111 (Donor)	NZ
LYS 31	NZ (Donor)	2.577	1.743	ASP 181 (Acceptor)	OD2

with Aß-HSP60 peptide using Cluspro 2.0. The help of binding residues then structurally visualized the immune response evoked and their bonding patterns by Aß-HSP60 peptide. The complications in developing a vaccine for specific disease like AD cannot be achieved through in silico studies, but efforts are made to simplify the time-consuming process in clinical trials through structural and sequential perspectives. Although the difficulties lie in treating AD, immunotherapy may be considered as a key factor. An ever-growing effort to apply computational methodologies having both biological and diagnostics knowledge may diminish the clinical complications in a viewpoint of molecular aspects.

Compliance with Ethical Standards

Conflict of interest All authors declare no competing financial interests in the findings of this study.

References

1. Paul S, Mahanta S (2014) Association of heat-shock proteins to various neurodegenerative disorders: is it a master key to open the therapeutic door? Mol Cell Biochem 386:45–61
2. Muchowski PJ (2002) Protein misfolding, amyloid formation, and neurodegeneration: a critical role for molecular chaperones? Neuron 35(1):9–12
3. Masters CL, Simms G, Weinman NA, Multhaup G, McDonald BL, Beyreuther K (1985) Amyloid plaque core protein in Alzheimer disease and Down syndrome. Proc Natl Acad Sci USA 82:4245–4249
4. Kang J, Lemaire HG, Unterbeck A, Salbaum JM, Masters CL, Grzeschik KH, Multhaup G, Beyreuther K, Muller-Hill B (1987) The precursor of Alzheimer's disease amyloid A4 protein resembles a cell-surface receptor. Nature 325:733–736
5. Jarrett JT, Berger EP, Lansbury PT (1993) The carboxy terminus of the beta amyloid protein is critical for the seeding of amyloid formation: implications for the pathogenesis of Alzheimer's disease. Biochemistry 32:4693–4697

6. Burdick D, Soreghan B, Kwon M, Kosmoski J, Knauer M, Henschen A, Yates J, Cotman Glabe C (1992) Assembly and aggregation properties of synthetic Alzheimer's A4/beta amyloid peptide analogs. J Biol Chem 267:546–554
7. Riek R, Guntert P, Dobeli H, Wipf B, Wuthrich K (2001) NMR studies in aqueous solution fail to identify significant conformational differences between the monomeric forms of two Alzheimer peptides with widely different plaque-competence, A beta(1–40)(ox) and A beta(1–42)(ox). Eur J Biochem 268:5930–5936
8. Tycko R (2004) Progress towards a molecular-level structural understanding of amyloid fibrils. Curr Opin Struct Biol 14:96–103
9. Kirschner DA, Abraham C, Selkoe DJ (1986) X-ray diffraction from intraneuronal paired helical filaments and extraneuronal amyloid fibers in Alzheimer disease indicates cross-beta conformation. Proc Natl Acad Sci USA 83:503–507
10. Balbach JJ, Petkova AT, Oyler NA, Antzutkin ON, Gordon DJ, Meredith SC, Tycko R (2002) Supramolecular structure in full-length Alzheimer's beta-amyloid fibrils: evidence for a parallel beta-sheet organization from solid-state nuclear magnetic resonance. Biophys J 83:1205–1216
11. Nussbaum JM, Seward ME, Bloom GS (2013) Alzheimer disease: a tale of two prions. Prion 7(1):14–19
12. Pulawski W, Ghoshdastider U, Andrisano V, Filipek S (2012) Ubiquitous amyloids. Appl Biochem Biotechnol 166(7):1626–1643
13. Parker MH, Reitz AB (2000) Assembly of β-amyloid aggregates at the molecular level. Chem Org Chem 13(1):51–56
14. Shankar GM, Li S, Mehta TH, Garcia-Munoz A, Shepardson NE, Smith I, Brett FM, Farrell MA, Rowan MJ, Lemere CA, Regan CM, Walsh DM, Sabatini BL, Selkoe DJ (2008) Amyloid β-protein dimers isolated directly from Alzheimer brains impair synaptic plasticity and memory. Nat Med 14(8):837–842
15. Prelli F, Castaño E, Glenner GG, Frangione B (1988) Differences between vascular and plaque core amyloid in Alzheimer's disease. J Neurochem 51(2):648–651
16. Hartl FU (1996) Molecular chaperones in cellular protein folding. Nature 381(6583):571–579
17. Lindquist S, Craig EA (1988) The heat shock proteins. Annu Rev Genet 22:631–677
18. Sherman MY, Goldberg AL (2001) Cellular defenses against unfolded proteins: a cell biologist thinks about neurodegenerative diseases. Neuron 29(1):15–32
19. Muchowski PJ, Wacker JL (2005) Modulation of neurodegeneration by molecular chaperones. Nat Rev Neurosci 6(1):11–22
20. Turturici G, Sconzo G, Geraci F (2011) Hsp70 and its molecular role in nervous system diseases. Biochem Res Int doi:10.1155/2011/618127
21. Cheng MY, Hartl FU, Horwich AL (1990) The mitochondrial chaperonin HSP60 is required for its own assembly. Nature 348(6300):455–458
22. Fenton WA, Kashi Y, Furtak K, Horwich AL (1994) Residues in chaperonin GroEL required for polypeptide binding and release. Nature 371:614–619
23. Ranford JC, Coates AR, Henderson B (2000) Chaperonins are cell-signalling proteins: the unfolding biology of molecular chaperones. Expert Rev Mol Med 2:1–17
24. Nemirovsky A, Fisher Y, Baron R, Cohen IR, Monsonego A (2011) Aß-HSP60 peptide conjugate vaccine treats a mouse model of Alzheimer's disease. Vaccine 29(23):4043–4050
25. Vellas B, Black R, Thal LJ, Fox NC, Daniels M, McLennan G, Tompkins C, Liebman C, Pomfret M, Grundman AN, 1792(QS-21)-251 study team (2009) Long-term follow-up of patients immunized with an1792: reduced functional decline in antibody responders. Curr Alzheimer Res 6(2):144–151
26. UniProt C (2009) The universal protein resource (UniProt) in 2010. Nucleic Acids Res 38:D142–D148. doi:10.1093/nar/gkp846
27. Hubbard TJ, Ailey B, Brenner SE, Murzin AG, Chothia C (1999) SCOP: a structural classification of proteins database. Nucleic Acids Res 27(1):254–256
28. Berman HM, Westbrook J, Feng Z, Gilliland G, Bhat TN, Weissig H, Shindyalov IN, Bourne PE (2000) The protein databank. Nucleic Acids Res 28(1):235–242
29. Altschul SF, Gish W, Miller W, Myers EW, Lipman DJ (1990) Basic local alignment search tool. J Mol Biol 215:403–410
30. Schwede T, Kopp J, Guex N, Peitsch MC (2003) SWISS-MODEL: an automated protein homology-modeling server. Nucleic Acids Res 31(13):3381–3385
31. Arnold K, Bordoli L, Kopp J, Schwede T (2009) The SWISS-MODEL workspace: a web-based environment for protein structure homology modelling. Bioinformatics 22(2):195–201
32. Wiederstein M, Sippl MJ (2007) ProSA-web: interactive web service for the recognition of errors in three-dimensional structures of proteins. Nucleic Acids Res 35:W407–W410
33. Sippl MJ (1993) Recognition of errors in three-dimensional structures of proteins. Proteins 17:355–362
34. Syed R, Rani R, Sabeena TA, Masoodi G, Shafi K, Alharbi K (2012) Functional analysis and structure determination of alkaline protease from Aspergillus flavus. Bioinformation 8(4):175–180
35. Pettersen EF, Goddard TD, Huang CC, Couch GS, Greenblat DM, Meng EC, Ferrin TE (2004) UCSF Chimera visualization system for exploratory research and analysis. J Comput Chem 25(13):1605–1612
36. Berendsen HJC, Van der Spoel D, Van Drunen R (1995) GROMACS: a message-passing parallel molecular dynamics implementation. Comput Phys Commun 91:43–56
37. Lindahl E, Hess B, Van Der Spoel D (2001) GROMACS 3.0: a package for molecular simulation and trajectory analysis. J Mol Model 7:306–317
38. Van der Spoel D, Lindahl E, Hess B, Groenhof G, Mark AE, Berendsen HJC (2005) GROMACS: fast, flexible, and free. J Comput Chem 26:1701–1718
39. Hess B, Kutzner C, Van der Spoel D, Lindahl E (2008) GROMACS 4: algorithms for highly efficient, load-balanced, and scalable molecular simulation. J Chem Theory Comput 4:435–447
40. Pandini A, Formili A, Fraternali F, Kleinjung J (2013) GSA-Tools: analysis of allosteric communication and functional local motions using a structural alphabet. Bioinformatics 29:2053–2055
41. Páll S, Abraham MJ, Kutzner C, Hess B, Lindahl E (2015) Tackling exascale software challenges in molecular dynamics simulations with GROMACS. EASC 2014. LNCS 8759:3–27
42. Meng EC, Pettersen EF, Couch GS, Huang CC, Ferrin TE (2006) Tools for integrated sequence-structure analysis with UCSF Chimera. BMC Bioinformatics 7:339
43. Kozakov D, Beglov D, Bohnuud T, Mottarella S, Xia B, Hall DR, Vajda S (2013) How good is automated protein docking? Proteins: structure, Function, and Bioinformatics. Proteins 81(12):2159–2166
44. Kozakov D, Brenke R, Comeau SR, Vajda S (2006) PIPER: an FFT-based protein docking program with pairwise potentials. Proteins 65:392–406
45. Comeau SR, Gatchell DW, Vajda S, Camacho CJ (2004) ClusPro: an automated docking and discrimination method for the prediction of protein complexes. Bioinformatics 20(1):45–50
46. Comeau SR, Gatchell DW, Vajda S, Camacho CJ (2004) ClusPro: a fully automated algorithm for protein–protein docking. Nucleic Acids Res 32:W96–W99

47. Mandell JG, Roberts VA, Pique ME, Kotlovyi V, Mitchell JC, Nelson E, Tsigelny I, Ten Eyck LF (2001) Protein docking using continuum electrostatics and geometric fit. Protein Eng 14:105–113
48. Chen R, Weng Z (2003) A novel shape complementarity scoring function for protein–protein docking. Proteins 51:397–408
49. Kolaskar AS, Tongaonkar PC (1990) A semi-empirical method for prediction of antigenic determinants on protein antigens. FEBS Lett 276(1–2):172–174
50. Sturniolo T, Bono E, Ding J, Raddrizzani L, Tuereci O, Sahin U, Braxenthaler M, Gallazzi F, Protti MP, Sinigaglia F, Hammer J (1999) Generation of tissue-specific and promiscuous HLA ligand database using DNA microarrays and virtual HLA class II matrices. Nat Biotechnol 17:555–561
51. Singh H, Raghava GPS (2001) ProPred: prediction of HLA-DR binding sites. Bioinformatics 17(12):1236–1237
52. Jeffrey GA (1997) An introduction to hydrogen bonding, Oxford University Press, Oxford, ISBN-10: 0195095499
53. Wallace AC, Laskowski RA, Thornton JM (1996) LIGPLOT: a program to generate schematic diagrams of protein-ligand interactions. Protein Eng 8:127–134
54. Shapovalov MS, Dunbrack RL Jr (2011) A smoothed backbone-dependent rotamer library for proteins derived from adaptive kernel density estimates and regressions. Structure 19:844–858
55. Geourjon C, Deleage G (1995) SOPMA: significant improvements in protein secondary structure prediction by consensus prediction from multiple alignments. Comput Appl Biosci 11(6):681–684
56. Reche PA, Glutting JP, Zhang H, Reinherz EL (2004) Enhancement to the RANKPEP resource for the prediction of peptide binding to MHC molecules using profiles. Immunogenetics 56(6):405–419
57. Murthy VL, Stern LJ (1997) The class II MHC protein HLA-DR1 in complex with an endogenous peptide: implications for the structural basis of the specificity of peptide binding. Structure 5(10):1385–1396